

Pseudogaps in Underdoped Cuprates

Patrick A. Lee

Department of Physics, Massachusetts Institute of Technology, Cambridge, MA 02139

It has become clear in the past several years that the cuprates show many unusual properties, both in the normal and superconducting states, especially in the underdoped region. In particular, gap-like behavior is observed in magnetic properties, *c*-axis conductivity and photoemission, whereas in-plane transport properties are only slightly affected by the pseudogap. I shall argue that these experimental evidences must be viewed in the context of the physics of a doped Mott insulator and that they support the notion of spin charge separation. I shall review recent theoretical developments, concentrating on studies based on the *t*-*J* model. I shall describe a model based on quasiparticle excitations, which predicts the doping dependence of T_c and anomalous energy-gap-to- T_c ratios. Finally, I shall outline how the model may be derived from a microscopic formulation of the *t*-*J* model. After a brief review of the $U(1)$ formulation, I shall explain some of the difficulties encountered there, and how a new $SU(2)$ formulation can resolve some of the difficulties.

I. INTRODUCTION

It has become clear in the past several years that the cuprates show many highly unusual properties both in the normal and superconducting (SC) states. These unusual features are related to the fact that the cuprates are doped Mott insulators. It is then not surprising that the unusual behaviors are most striking in the underdoped region, when the concentration of doped holes, x is small. In the normal state a pseudogap is observed in a temperature range considerably above the SC transition temperature T_c . The gap is seen in NMR relaxation rate $1/T_1$, Knight shift [1] and specific heat. [2] It is also seen in *c*-axis conductivity [3] and in photoemission experiments [4,5] which reveal that the pseudogap is roughly of the same size and \mathbf{k} dependence as the *d*-wave SC gap. Furthermore, the gap size is essentially independent of x and even increases slightly when T_c is reduced with decreasing x . This observation is also supported by tunneling data. [6] On the other hand, the in-plane transport properties are only slightly affected by the pseudogap. The resistivity shows a small decrease which may be interpreted as a decrease in the scattering rate. [7] More importantly, the spectral weight of the Drude part of $\sigma(\omega)$ is proportional to x [8] and there is no evidence that it is strongly reduced by the presence of the pseudogap. [7,9,10] We believe this is strong experimental evidence supporting the notion of spin-charge separation [11] in these materials. It was pointed out by P.W. Anderson [11] early on that the Néel state is not the best way to accommodate the competition between the hole kinetic energy and the spin exchange energy. He envisioned another possibility, i.e., the spins form a liquid of singlets, which he termed the resonating valence bond (RVB) state. The reason is that the energy to form a singlet $-JS(S+1)$ is particularly favorable for $S = \frac{1}{2}$. The holes can move more freely among the liquid of singlets and are responsible for the charge transport. This no-

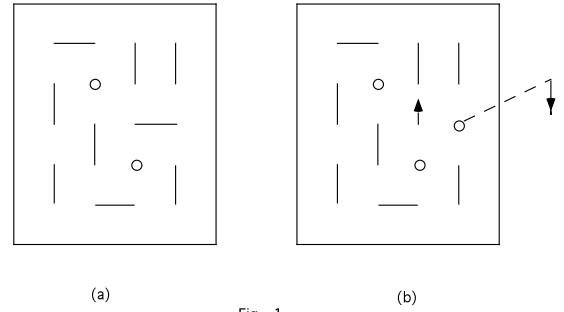


Fig. 1

FIG. 1. A cartoon representation of the RVB liquid or singlets. Solid bond represents a spin singlet configuration and circle represents a vacancy. In Fig. (1b) an electron is removed from the plane in photoemission or *c*-axis conductivity experiment. This necessitates the breaking of a singlet.

tion of spin charge separation naturally accounts for all the qualitative features of the spin gap state noted above. The spins form RVB singlets so that it costs energy (spin gap) to make triplet excitations. However the in-plane conductivity is carried by x holes, which remain gapless. In *c*-axis conductivity and photoemission, a physical electron is removed from the plane, which carries both spin and charge. It then follows that the spin gap should appear in these experiments. This picture is illustrated in Fig. 1.

We note that an alternative model which exhibits the above phenomenology is the model of preformed pairs above T_c . There are two versions of this class of model; the first suggests that strong phase fluctuation [12] destroys long range order over a large temperature range above T_c , and the second assumes that we are in the short coherence length limit of the pairing state [13], so that essentially pair “molecules” are first formed and then Bose condensed. [14,15] The phase fluctuation model predicts that the pairing amplitude is responsible for the pseudogap and would seem to predict that other manifestations

of superconductivity such as conductivity and diamagnetism fluctuations should be observable, particularly at short distance and short time scale. A recent high frequency conductivity experiment in underdoped BISCO [16] shows that while Berenzinskii-Kosterlitz-Thouless (BKT) type fluctuations are observed near and above T_c , the short distance (bare) superfluid density extracted from these measurements vanishes above 100 K, much below the temperature range associated with the pseudogap. These data are difficult to understand within the phase fluctuation model. Similarly, in the short coherence length model, charge transport is by charge $2e$ pairs in the pseudogap state and it is difficult to understand the insensitivity of the transport properties to the appearance of the pseudogap with underdoping. Furthermore, it is not at all clear that the coherence length is short in the underdoped limit. In section III we shall in fact argue that the coherence length increases with underdoping, and that one is not in the short coherence length regime. In any event, in both these models a superconducting state with a large energy gap is postulated to exist, without any indication of the origin and the energy scale of the gap. The RVB picture is fundamentally different from these preformed pair pictures in that spin-charge separation plays a crucial role. The pseudogap is a spin gap with an energy scale set by J , which becomes the superconducting gap with the onset of coherence in the charge degrees of freedom. The superconducting state is characterized by spin-charge recombination, forming superconducting quasiparticles which are quite conventional in the BCS sense.

We model the cuprate with the t - J model, which we believe contains the essential physics of the doped Mott insulator. The t - J Hamiltonian is

$$H = \sum_{\langle ij \rangle} J \left(\mathbf{S}_i \cdot \mathbf{S}_j - \frac{1}{4} n_i n_j \right) - t \sum_{\sigma} (c_{\sigma i}^{\dagger} c_{\sigma j} + h.c.)$$

is subject to the constraint that double occupancy of a site by two electrons of opposite spins is not allowed. Here $\mathbf{S}_i = c_{i\alpha}^{\dagger} \boldsymbol{\sigma}_{\alpha\beta} c_{i\beta}$ and $n_i = \sum_{\alpha} c_{i\alpha}^{\dagger} c_{i\alpha}$. The t - J model is the strong coupling limit of the Hubbard model and the difficulty of its solution lies in enforcing the no double occupancy constraint. For the cuprates the parameters are known to be $J \approx 0.13$ meV and $t/J \approx 3$. When holes are doped into the insulator, there is a gain in kinetic energy per hole proportional to t due to hopping. However, the spin correlation is destroyed, costing an energy of approximately J per site. Thus we can consider the doping problem as a competition between the energy xt (kinetic energy per site) and J . When $xt \ll J$, the AF state with its doubled unit cell is retained and the holes form small pockets around the top of the single hole dispersion, which is known to be at $(\pi/2, \pm\pi/2)$ from photoemission [17] (see Fig. 2). This problem belongs to the same class as the doping of a band insulator

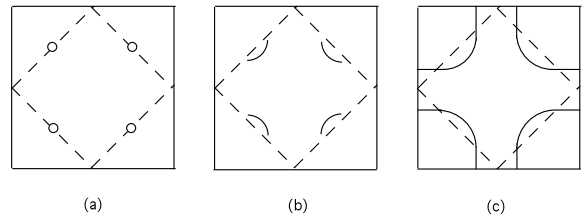


Fig. 2

FIG. 2. The evolution of the locus of low lying single particle excitation with doping. (a) low doping AF state: Brillouin zone is doubled with small hole pockets of area x . (b) underdoped: Fermi surface “segments.” (c) overdoped: Fermi surface with area $1 - x$, satisfying Luttinger theorem.

(or semiconductor). The only difference is that the coherent part of the band has a reduced spectral weight of J/t and a bandwidth of order J . This can be understood in terms of a spin-polaron picture, i.e., the hopping hole is surrounded by a cloud of spin excitations. [18] On the other hand, if $xt \gg J$, the spin correlation becomes unimportant, AF order is destroyed, and the holes should form a metallic state, describable by Fermi liquid theory. The Luttinger theorem then dictates that the area of the Fermi surface is given by $1 - x$, as shown in Fig. 2c. The important point is the electrons which form the local moments in the Mott insulator are now mobile and should be counted as part of the Fermi sea. The change in Fermi surface area from x to $1 - x$ between the low and high doping limit is a special feature of the doping of a Mott insulator, associated with the liberation of the local moments. The question then arises: how does the system evolve between these two limits? The intermediate state is apparently the spin gap state, with gaps in the one electron spectrum in the vicinity of $(0, \pi)$ and segments of the Fermi surface near $(\pi/2, \pi/2)$ (see Fig. 2b). As doping is increased, these segments grow in length and eventually join to form the Luttinger Fermi surface. This intermediate state is clearly not a Fermi liquid because in band theory, gapping of parts of the Fermi surface is not permitted without symmetry breaking. However, the breakdown of Fermi liquid theory is not a sharply posed issue at finite temperatures. The existence of the superconducting ground state at intermediate doping means that this question cannot be investigated experimentally at present. It is worth noting that the transition region occurs near $x = 0.2$, when xt and J are comparable.

We emphasize once again that an important aspect of the doping of the Mott insulator is that the resulting metal must remember that x holes are responsible for the electrical conductivity. If the AC conductivity $\sigma(\omega)$ is characterized by a Drude-like component at low frequency, we may characterize the conductivity by the scattering rate $1/\tau$ and the spectral weight $(n/m)_{\text{effective}}$. For underdoped samples, this spectral weight is propor-

tional to x . [8] This is very natural in that the weight must vanish when $x \rightarrow 0$. It follows that a superconductor that forms out of the underdoped metal must have a superfluid density ρ_s given by this spectral weight (in the clean limit), so that ρ_s is proportional to x . This simple observation will play a prominent role in our subsequent discussion. On the other hand, when $xt > J$ we have a Fermi liquid state with electron density $1 - x$. The question then arises as to how $(n/m)_{\text{effective}} \approx x$ can be accommodated within Fermi liquid theory. Within Fermi liquid theory we can write

$$\left(\frac{n}{m}\right)_{\text{effective}} = \frac{1-x}{m^*} \left(1 + \frac{F_{1S}}{2}\right) \quad (1)$$

where m^* is the effective mass and F_{1S} is a Landau parameter. It describes the deviation of the current carried by the quasiparticle from $-e\mathbf{v}_{\mathbf{k}}$ due to dragging of other quasiparticles

$$\mathbf{j} = -e\alpha\mathbf{v}_{\mathbf{k}} \quad (2)$$

where $\alpha = (1 + F_{1S}/2)$. [19] Here we have made the simplifying assumption that only the $\ell = 1$ Landau parameter (in 2d) is important and the correction is independent of \mathbf{k} . From Eq. (1) we see that there are two ways to obtain $(n/m)_{\text{eff}} = x$. The first is to generate a heavy mass so that $m^* = 1/x$. This is in fact the case for the system $\text{La}_{1-x}\text{Sr}_x\text{TiO}_3$ which is a Mott insulator for $x = 0$ with a Néel temperature of $T_N = 150$ K. With doping $x > 0.02$, a metallic state is formed with the spin susceptibility χ and the specific heat coefficient γ both scaling as $1/x$ and a Wilson ratio of order unity. [20] The Hall coefficient $R_N \sim 1/(1-x)$ as expected for a Fermi surface dictated by Luttinger theorem. This is clearly a realization of the Fermi liquid state expected for $xt > J$. Unlike the cuprates, LaTiO_3 is a three dimensional system, so that the exchange constant J can be deduced from the ordering temperature. Thus the ratio J/t is very small and we believe this is the reason why the Fermi liquid state persists to low doping. For $x < 0.02$, disorder effects become important and we are not able to explore the $xt < J$ limit in this system.

A second route to achieve a spectral weight of x is for $(1 + \frac{F_{1S}}{2}) \approx x$. It turns out this is the route followed by the mean field slave boson theory described below. [21] We shall see that in the underdoped region this route is not followed in the cuprate system. We have strong evidence that the factor α in Eq. (2) is not proportional to x and is in fact of order unity.

II. MICROSCOPIC MODEL AND MEAN FIELD THEORY

The physics of spin charge separation appears naturally in a class of theory which starts with the t - J model

and enforces the constraint of no double occupation by decomposing the electron into a fermion and a boson, $c_{i\sigma}^\dagger = f_{i\sigma}^\dagger b_i$. The fermion $f_{i\sigma}$ carries spin index and the boson b_i keeps track of the charge degrees of freedom. The constraint is replaced by the requirement that $f_{i\sigma}^\dagger f_{i\sigma} + b_i^\dagger b_i = 1$ which can be enforced by introducing a Lagrangian multiplier so that field theoretic methods may be applied. This decomposition (called the slave boson method) is not unique and one could just as well associate the spin with the boson (the Schwinger boson theory [22]). If the theories are solved exactly they should give identical results. However, different factorization leads naturally to different approximation schemes. Our strategy is to explore the different schemes to see which correspond most closely with experiment. In particular, while the Schwinger boson method gives an excellent description of the antiferromagnetic state at half filling, [22] it does not produce a large Fermi surface for large doping. Since we are mainly interested in the regime of intermediate doping, the slave boson is a more promising starting point.

The exchange term can be written in terms of the fermions only [23]

$$\begin{aligned} J \vec{S}_i \cdot \vec{S}_j &= -J \left| f_{i\alpha}^\dagger f_{j\alpha} \right|^2 \\ &= -J \left(f_{i\uparrow}^\dagger f_{j\downarrow}^\dagger - f_{i\downarrow}^\dagger f_{j\uparrow}^\dagger \right) (f_{i\downarrow} f_{j\uparrow} - f_{i\uparrow} f_{j\downarrow}) \end{aligned} \quad (3)$$

which invites the following mean field decoupling

$$\begin{aligned} \chi_{ij} &= \langle f_{i\sigma}^\dagger f_{j\sigma} \rangle \quad \text{and} \\ \Delta_{ij} &= \langle f_{i\uparrow}^\dagger f_{j\downarrow}^\dagger - f_{i\downarrow}^\dagger f_{j\uparrow}^\dagger \rangle \end{aligned} \quad (4)$$

These parameters describe the formation of a singlet on the bond ij . The mean field phase diagram [24,25] is shown schematically in Fig. 3. As the temperature is lowered, $\chi_{ij} \neq 0$, so that the fermions now acquire an energy band and a Fermi surface. At a lower temperature, the fermions form a pairing state with d -wave symmetry. The bosons become essentially Bose condensed (with exponentially large correlation length with decreasing T) below a cross-over temperature $T_{BE}^{(0)} = 2\pi xt$. Below $T_{BE}^{(0)}$ the boson field can be treated as a c -number. In the overdoped region this gives rise to a Fermi liquid phase, similar to the theory of heavy fermion systems. In the intermediate doping range, the simultaneous presence of Δ_{ij} and $\langle b \rangle$ gives rise to a pairing order parameter for physical electrons $\langle c_{i\uparrow} c_{j\downarrow} \rangle$ which is of d -wave symmetry. Above $T_{BE}^{(0)}$ spin charge separation occurs at the mean field level. In the pairing state a d -wave type gap occurs in the spin excitation spectrum, but not in the charge excitation, and it is natural to identify this as the spin gap phase. Finally, the region IV in Fig. 3 is a non Fermi liquid state which may be referred to as a “strange metal.”

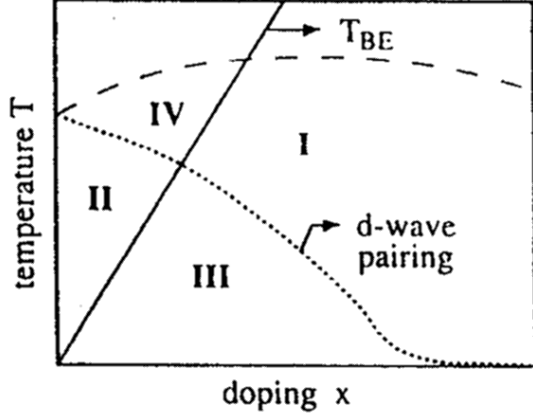


FIG. 3. Schematic mean-field phase diagram of the t - J model. Below the dashed line the uniform RVB order parameter χ_{ij} is nonzero. The mean-field pairing line below which $\Delta_{ij} \neq 0$ (dotted) and the Bose-condensation line (solid) divide the phase diagram into four regions. Region I is a Fermi-liquid phase, region II is the spin-gap phase, region III is the superconducting phase, and region IV is the strange metal phase.

We can go beyond mean field to include fluctuations about the mean field solution. The most important fluctuations are the phase fluctuations of the order parameter $\chi_{ij} = |\chi_{ij}|e^{i\theta_{ij}}$. Particles hopping around a plaquette acquire a phase related to θ_{ij} , just like electrons in the presence of a magnetic flux. These low lying excitations are $U(1)$ gauge fields. [26] We shall refer to this theory as the $U(1)$ formulation. When coupled to the fermions and bosons they enforce the constraint locally, not just on average as in mean field theory.

III. PHENOMENOLOGICAL DESCRIPTION OF THE SUPERCONDUCTING STATE

Before continuing with the microscopic theory, we digress to review a phenomenological description of the superconducting state. [27] The idea is to start at low temperature where the nature of the elementary excitations is well understood, and calculate the reduction of the superfluid density with increasing temperature. This can be done by making two assumptions: A) the superfluid density is given by x , and B) the quasiparticle (qp) dispersion in presence of an external electromagnetic gauge potential has a BCS form:

$$E_{\mathbf{A}}^{(sc)}(\mathbf{k}) = \pm \sqrt{\varepsilon^2(\mathbf{k}) + \Delta^2(\mathbf{k})} + \frac{\mathbf{A}}{c} \cdot \mathbf{j}(\mathbf{k}) \quad (5)$$

for \mathbf{k} near the nodes, where $\mathbf{j}(\mathbf{k})$ is given by Eq. (2). Note that $\mathbf{v}_F \equiv \partial_{\mathbf{k}}\varepsilon$ is the “normal state” Fermi velocity and that the vector potential \mathbf{A} couples only through the “normal state dispersion” $\varepsilon(\mathbf{k})$ and has nothing to

do with the SC gap $\Delta(\mathbf{k})$. The physical reason for this is that this quasiparticle is a superposition of an electron with momentum \mathbf{k} and a hole with momentum $-\mathbf{k}$, and both these objects carry the same charge current $\mathbf{j}(\mathbf{k})$. Mathematically Eq. (5) is easily derived by noting that \mathbf{A} enters only in the diagonal elements of the BCS matrix in the form $\varepsilon(\mathbf{k} + \mathbf{A}) - \mu$ and $-\varepsilon(-\mathbf{k} + \mathbf{A}) - \mu$, which is diagonalized to give Eq. (5) to linear order in \mathbf{A} .

With these assumptions we can calculate how the superfluid density is reduced by thermal excitation of quasiparticles. We found that

$$\frac{\rho_s}{m}(T) = \frac{x}{a^2 m} - \frac{2\alpha^2 \ln 2}{\pi} \frac{v_F}{v_2} T \quad (6)$$

where $v_2 = \Delta_0 a / \sqrt{2}$ is the velocity of the quasiparticle in the direction of the maximum gap Δ_0 , i.e., in the direction from the node towards $(0, \pi)$. The ratio v_F/v_2 thus measures the anisotropy of the massless Dirac cone which characterizes the d -wave qp spectrum.

Based on numerical calculations and theoretical considerations, [28,29] we expect the mass m in Eq. (6) to correspond to a tight-binding hopping integral of order t so that $m^{-1} \sim t$. Experimentally it is found that m is about twice the electron mass [8], which happens to correspond to a hopping integral of $J \approx 0.13$ eV. We believe that the theoretical expression for the hopping integral is $t/3$ which happens to equal J in our case. On the other hand, the Fermi velocity v_F is proportional to the coherent bandwidth, which is given by J . To keep our expression general, we keep track of the distinction between $t/3$ and J , even though numerically they are equal.

We see that for small x , the quasiparticle excitation is an effective way of destroying the superconducting state by deriving ρ_s to zero. By extrapolating Eq. (6) to $\rho_s = 0$, we can estimate T_c as being of order

$$T_c \approx x \Delta_0 (t/3J) . \quad (7)$$

Note that this is a violation of the BCS ratio $2\Delta_0/kT_c = \text{constant}$. Presumably the real transition is driven by critical fluctuations including phase fluctuations and vortex unbinding in the 2d limit, but the underlying (bare) superfluid density should be driven to zero by quasiparticle excitations in the way we indicate. There is experimental support for this point of view from high frequency conductivity measurements. [16] If we further assume that Δ_0 is independent of x for underdoped cuprates, we see that T_c is proportional to x (or more precisely to $\rho_s(T=0)/m$), thus providing an explanation of Uemura’s plot. [14]

It is worth noting that in the slave boson mean field theory Δ_0 is proportional to J , since that is the only energy scale relevant to the formation of spin singlets. Then Eq. (7) predicts that T_c is proportional to xt . Apart from numerical coefficients, this has the same functional

dependence as the Bose condensation temperature $T_{BE}^{(0)}$, as well as the transition temperature based on pairing of bosons to be discussed later in the $SU(2)$ formulation.

Another important implication is that superconductivity is destroyed when only a small fraction of the quasiparticles (with energy $\leq x\Delta_0$) are thermally excited. Thus the gap near $(0, \pi)$ must remain intact in the normal state, leaving a strip of thermal excitations which extend a distance proportional to x from the nodal points. This is qualitatively in agreement with the photoemission experiment. Of course our phenomenological picture does not provide a description of the normal state. It simply states that the normal state gap is an inescapable consequence of a finite Δ_0 and a vanishingly small superfluid density as $x \rightarrow 0$.

The fact that $d\rho_s/dT$ is independent of x and that both ρ_s and T_c are proportional to x means that a scaled plot of $\rho_s(T)/\rho_s(0)$ vs T/T_c should be independent of x for small T/T_c . In fact, such a scaled plot for YBCO_{6.95} and YBCO_{6.60} shows a remarkable universality over the entire temperature range. [30] We can use the data to extract the ratio $\alpha^2 v_F/v_2$ using Eq. (4). Using the YBCO_{6.95} data, we obtain a velocity anisotropy $v_F/v_2 = 6.8$ if we assume that $\alpha = 1$. [27]

Alternatively, by comparing the measured slope $d\rho_s/dT$ of the YBCO_{6.95} and YBCO_{6.60} samples, we see that the slopes are almost the same, showing that $\alpha^2 v_F/v_2$ is almost independent of doping. From tunneling data we know that the maximum gap Δ_0 slightly increases with underdoping. [6] This implies that α is almost independent of x . This is the experimental evidence that the Fermi liquid scenario $\alpha = x$ does not apply to the underdoped cuprates.

It is useful to compare Eq. (4) with the standard BCS expression which is usually written in the form [31]

$$\rho_s(T) = \rho_s(0) \left(1 - \frac{(2 \ln 2)T}{\Delta_0} \right) \quad (8a)$$

$$= \rho_s(0) - \rho_s(0)(2 \ln 2)T/\Delta_0 \quad (8b)$$

This expression does not include Fermi liquid correction and should be compared with Eq. (6) with $\alpha = 1$. We note that in BCS theory $\rho_s(0)$ is independent of x and the second term in Eq. (8) is in exact agreement with the second term in Eq. (6) as it should be, because the derivation leading to Eq. (6) is completely general. The first terms in Eq. (8) and Eq. (6) do not agree because the standard BCS theory does not apply to a doped Mott insulator and does not include the physics leading to a spectral weight proportional to x . It is clear that this feature of Eq. (8) does not agree with experiment on underdoped cuprates. If one ignores this and fits the normalized data $\rho_s(T)/\rho_s(0)$ to Eq. (8a), one would reach the incorrect conclusion that the energy gap Δ_0 is proportional to T_c in underdoped cuprates. [32] We emphasize that Eq. (6) includes Eq. (8) as a special case and must be used in

place of Eq. (8) for a correct analysis of the data.

We can also estimate the size of the vortex core using this picture. The idea is to identify the core size as the point where the critical current is reached. If we replace $-e\mathbf{A}/c$ in Eq. (2) by the gauge invariant superfluid velocity $\mathbf{v}_s = \frac{1}{2}(\nabla\theta - \frac{2e}{c}\mathbf{A})$, we see that the quasiparticle energy shifts up or down in the presence of v_s and quasiparticles are generated at the Fermi energy, contributing to a normal fluid density. Near the vortex core, v_s grows as $1/R$, so that the normal fluid density grows and eventually drives the critical current to zero. This allows us to estimate the core size to be

$$R_1 \approx \frac{1}{x} \frac{v_F}{\pi \Delta_0 (t/3J)} \approx \frac{v_F}{\pi T_c} \quad (9)$$

Note the factor x appears in the denominator. We note that in BCS theory, the coherence length can be written either as $v_F/\pi T_c$ or v_F/Δ_0 . The two forms are equivalent because the ratio $2\Delta_0/kT_c$ is a constant. In our case this ratio depends on x and it is not clear *a priori* which form is correct for the coherence length. Equation (9) shows that $v_F/\pi T_c$ is the correct form for the coherence, and not $v_F/\pi \Delta_0$. One consequence of this is that the underdoped cuprates are in fact not short coherence length superconductors. [15] The number of holes per coherence volume actually grows as x^{-1} with decreasing doping. A second consequence is that H_{c2} (due to orbital effects) is predicted to scale as x^2 . Within this picture it is also clear that in underdoped cuprates the state inside the vortex core should retain the large gap Δ_0 , just as the normal state above T_c .

We can now estimate the condensation energy using the relation $\Delta E = H_c^2/8\pi$ and $H_c^2 = H_{c1}H_{c2}$. Noting that H_{c1} is proportional to $\rho_s(0)/m \approx xt$ while $H_{c2} = \phi_0/R_1^2$ is proportional to x^2 , we find that ΔE is proportional to x^3 , i.e.,

$$\Delta E \approx x(T_c^2/J)(t/3J) \quad (10)$$

This is in contrast to the BCS expression $\Delta E \approx T_c^2/\epsilon_F$. Equation (10) also follows from a picture where only the quasiparticles with energy less than T_c are affected by the transition to the normal state. The area of the Brillouin zone occupied by these excitations is of order $(T_c/J)(T_c/\Delta_0)$, so the total energy change per area is of order $T_c^3/J\Delta_0$ which agrees with Eq. (10). Thus even when expressed in terms of T_c the condensation energy is much less than the BCS value in the underdoped system. There is evidence for this suppression of the condensation energy from specific measurements. [2]

IV. THE $SU(2)$ FORMULATION OF THE T-J MODEL

We now return to discuss the microscopic theory. While the mean field phase diagram is in qualitative

agreement with experiments, the $U(1)$ formulation suffers from a number of deficiencies if we try to improve the mean field theory by including gauge fluctuations at the Gaussian level. In the spin gap phase the problem lies with the fact that the MF theory is a pairing theory of fermions and carriers with it some features of superconductivity. For example, the gauge field is gapped by the fermion pairing via the Anderson-Higgs mechanism. This leads to a reduction of gauge fluctuations which actually destabilize the pairing phase. [33] A second problem is that if we introduce residual interaction between the fermions and bosons to form an electron, the electron spectrum will always have nodes. This is because the node structure in the pairing state is tied to the Fermi level and is very resilient to interactions. Thus we have difficulty reproducing the “Fermi surface segments” which are apparently observed in photoemission experiments. In the superconducting phase we have condensation of the bosons and the quasiparticles become well defined. While this feature is in agreement with experiment, the current carried by the quasiparticles turns out to be reduced so that in Eq. (2), $\alpha = x$. As we have seen, this leads to a serious disagreement with the doping dependence of the temperature coefficient of the London penetration depth. In order to circumvent these difficulties, we were led to a new formulation of the t - J model which is designed to be more accurate near half filling. We briefly outline the $SU(2)$ formulation below. [34,35]

In this new formulation we introduce an $SU(2)$ doublet of boson fields $b^T = (b_1, b_2)$, in addition to the fermion doublet $\psi^\dagger = (\psi_\uparrow, \psi_\downarrow)$. The physical electron is represented by the $SU(2)$ singlet formed out of these two doublets, $c_\uparrow = \frac{1}{\sqrt{2}}b^T\psi$, $c_\downarrow = \frac{1}{\sqrt{2}}b^\dagger\bar{\psi}$ where $\bar{\psi} = i\tau^2\psi^*$. We are motivated by the observation made by Affleck *et al.* [36] that at half-filling ($x = 0$) the fermion representation of the t - J model has the $SU(2)$ symmetry in that a spin-up electron can be represented by a spin-up fermion or the absence of a spin-down fermion. In the $U(1)$ formulation this symmetry is broken as soon as $x \neq 0$, and out of a infinite degeneracy of states, the d -wave fermion pairing state is picked out as the MF solution. In contrast, even at the mean field level, the low lying states which are missing in the $U(1)$ mean field theory are included in the new $SU(2)$ formulation. For example, the spin gap state can be described equally well as the d -wave pairing state, or a staggered flux phase, where the fermions see gauge fluxes which alternate from plaquette to plaquette. The $SU(2)$ gauge transformation relates these states and guarantees that there is no breaking of the translational symmetry. The fermion spectrum exhibits a d -wave type gap, with maximum gap at $(\pi, 0)$ and nodes at $(\pi/2, \pi/2)$. We compute the physical electron spectral function, which at the mean field level, is a convolution between the fermion and boson spectra. We further introduced a residual interaction between the

fermions and bosons. The resulting spectra can be compared with photoemission experiments and have the following features. The spectra consist of a coherent part with spectral weight x and dispersion of order J and a broad incoherent part. The coherent part closely resembles the fermion dispersion. The residual interaction broadens and shifts the nodes at $(\pi/2, \pi/2)$ so that we obtain a “Fermi surface segment” near $(\pi/2, \pi/2)$. Away from this segment a gap appears in the excitation spectrum which grows to its maximal magnitude near $(0, \pi)$. This behavior is in qualitative agreement with the angle-resolved photoemission experiment. [4,5]

We have also studied the fermion spectrum and how it is affected by gauge fluctuations. We found a logarithmic correction to the fermion velocity and we successfully fitted the magnetic susceptibility and the specific heat in the spin gap state. [37]

In the superconducting state we need to address the issue of the current carried by the quasiparticles. To expand on this point further, we note that in the original $U(1)$ gauge field formulation of the t - J model, the prediction for $\rho_s(T)$ takes the form of Eq. (6) with $\alpha = x$ and therefore is in strong disagreement with experiment. This follows simply from the Ioffe-Larkin rule which states that the inverse of the response function of the fermion and boson should add to give the physical inverse response. In the superconducting state, the fermion and boson acquire superfluid densities ρ_F and ρ_s so that

$$\rho_s^{-1}(T) = \rho_F^{-1}(T) + \rho_B^{-1}(T) \quad (11)$$

where $\rho_F \approx (1 - x)$ and $\rho_B \approx x$. However, only the temperature dependence of ρ_F depends on the qp gap structure and is expected to be of the form $\rho_F(T) \approx (1 - x)(1 - T/\Delta_0)$, whereas the temperature dependence of ρ_B arises only through the excitation of sound mode and should be higher power in T , which can be ignored. Inserting these into Eq. (11) we see that $\rho_s(T)$ is predicted to be $x - x^2T/\Delta_0$. Basically in the $U(1)$ gauge theory the mismatch of the Fermi surface area and the Drude spectral weight (or ρ_s in the superconducting state) is solved by a Landau parameter, so that $\alpha = x$. Thus we may conclude that it is not sufficient to treat the gauge fluctuation only to quadratic order as in the Ioffe-Larkin theory.

We believe this difficulty is tied to the notion of Bose condensation as a way of achieving superconductivity. The reason is the following. The electron operator c_k is a convolution of the fermion and boson operator in momentum space. Let us suppose that the external \mathbf{A} field couples only to the boson (this is true in the $SU(2)$ formulation and is approximately true in some gauge choice in the $U(1)$ formulation). In the presence of \mathbf{A} , $b_{\mathbf{q}} \rightarrow b_{\mathbf{q}+\mathbf{A}}$ so that after the convolution $c_{\mathbf{k}} \rightarrow c_{\mathbf{k}+\mathbf{A}}$ and $\epsilon_{\mathbf{k}} \rightarrow \epsilon_{\mathbf{k}+\mathbf{A}}$ as expected. Thus $j_{\mathbf{k}} = -e\partial\epsilon/\partial\mathbf{A} = -e\partial\epsilon/\partial\mathbf{k}$. Let us see what happens in the superconducting state. If we

assume that the fermions are already paired, superconductivity can be driven by the condensation of bosons $\langle b_{\mathbf{k}=0} \rangle = 0$. However, in the presence of \mathbf{A} , the Bose condensate remains rigid and stays in the $k = 0$ state. This is clearly seen in the Ginsburg Landau theory for the free energy $|(\nabla - 2e\mathbf{A}/c)b|^2$ where $\langle b_{\mathbf{k}=0} \rangle \neq 0$ in the presence of \mathbf{A} is responsible for the Higgs mechanism and the London penetration depth. Upon convolution, we see that for the electron operator, \mathbf{k} is not shifted by \mathbf{A} so that $\epsilon(\mathbf{k})$ is independent of \mathbf{A} . The qp now carries no current! In the $U(1)$ formulation, the gauge field \mathbf{a} causes a small shift in the Fermion spectrum and leads to Eq. (2) with $\alpha = x$. This is clearly an unacceptable situation and can be seen most acutely for the qp at the Fermi surface along the (π, π) direction. Here the energy gap vanishes so that the qp in the superconducting state is basically the same state above T_c . Yet, according to the Bose condensation scenario, the current carried by this qp drops abruptly below T_c .

Now that we have identified the problem, we can see that there are two possible ways to avoid it. The first is to argue that due to fluctuations, only a small fraction of the bosons are in the condensate and we can reduce the problem, but not eliminate it. We call this the single boson condensation (SBC) scenario. The result is that α can lie anywhere between x and 1, and most likely somewhere in between. A second possibility is allowed in the $SU(2)$ formulatin but not in the $U(1)$ formulation. In $SU(2)$ theory there are two species of bosons b_1 and b_2 and we can pair them to form a gauge singlet pair $\langle b_1(\mathbf{i})b_2(\mathbf{j}) \rangle \neq 0$. We shall call this the boson pair condensation (BPC) scenario. Since $\langle b_1 \rangle = \langle b_2 \rangle = 0$, the problem is avoided and we find that $\alpha = 1$. This is really a consequence of continuity because in this scenario the superconducting qp along (π, π) is smoothly connected to the electron state above T_c . This result comes out of an explicit calculation which we outline below. [38]

In $SU(2)$ theory we go beyond MF theory by calculating the electron propagator through a ladder diagram [34,35] to include effects of pairing between the boson and the fermion. Here we will consider only the simplest on-site interaction $V(c_{\uparrow}^{\dagger}c_{\uparrow} + c_{\downarrow}^{\dagger}c_{\downarrow})$, which, when written in terms of bosons and fermions, generates an attraction between bosons and the fermions if $V > 0$. There are also other pairing interactions, but they will not modify our results qualitatively. The resulting electron propagator is given by

$$\mathbf{G}_{\mathbf{A}}(\omega, \mathbf{k}) \equiv \begin{pmatrix} -i\langle c_{\uparrow}^{\dagger}c_{\uparrow} \rangle & -i\langle c_{\uparrow}^{\dagger}c_{\downarrow} \rangle \\ -i\langle c_{\downarrow}^{\dagger}c_{\uparrow} \rangle & -i\langle c_{\downarrow}^{\dagger}c_{\downarrow} \rangle \end{pmatrix} \quad (12)$$

$$= \left[\begin{pmatrix} G_{0,\mathbf{A}}(\omega, \mathbf{k}) & F_{0,\mathbf{A}}(\omega, \mathbf{k}) \\ F_{0,\mathbf{A}}(\omega, \mathbf{k}) & -G_{0,\mathbf{A}}(-\omega, -\mathbf{k}) \end{pmatrix}^{-1} - V\tau^3 \right]^{-1} \quad (13)$$

We first consider the second scenario where there are no SBC, but there is a nonzero $F_{0,\mathbf{A}}$ proportional to

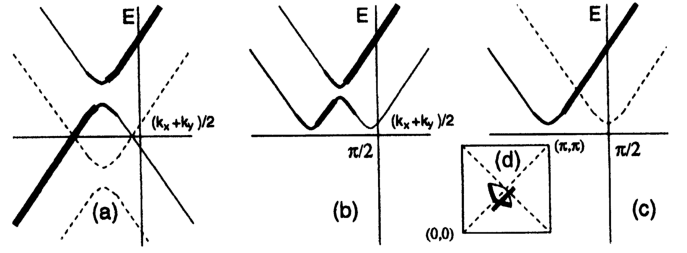


FIG. 4. Schematic illustration of the QP dispersion (the pole location of \mathbf{G} for (a) normal state, and SC state with (b) $0 < x_{pc} < x$ and (c) $x_{pc} = x$. The line thickness indicates the size of the residue of G_{11} , and the dashed line indicates vanishing residue. The momentum scan is along the straight line in (d), where the curved segment is the FS segment in the normal state.

the boson pair parameter x_{pc} . For $\mathbf{A} = 0$, the poles of $G_{11}(\omega, \mathbf{k})$ comes in pairs of opposite signs, just as in BCS theory. However the total residue is $\frac{x}{2(1-VG_{in})^2}$, significantly reduced from the BCS value. There are two positive branches which determine the qp excitations

$$E_{\pm}^{(sc)}(\mathbf{k}) = \sqrt{\tilde{E}_{\pm}^2 + \left(\frac{x_{pc}}{x}\Delta\right)^2} \quad (14)$$

where

$$\tilde{E}_{\pm} = \pm \sqrt{(\varepsilon - \tilde{\mu})^2 + \Delta^2 - \left(\frac{x_{pc}}{x}\Delta\right)^2} - \tilde{\mu} \quad (15)$$

and $\tilde{\mu} = -\frac{xV}{4(1-VG_{in})}$. In order to interpret those results, let us first consider the normal state which is recovered by setting $x_{pc} = 0$ in Eq. (14) and Eq. (15), yielding the normal state dispersion $E_{\pm}^N \equiv \tilde{E}_{\pm}(x_{pc} = 0)$. This corresponds to a massless Dirac cone initially centered at $(\pm\pi/2, \pm\pi/2)$ when $V = 0$ which is the MF fermion spectrum of the staggered-Flux (*s*-Flux) phase. The effect of V (the boson-fermion pairing) is two-fold. The $\tilde{\mu}$ inside the square-root shift the location of the node towards $(0, 0)$ by a distance $\Delta k = -\tilde{\mu}/v_F$ while the last term shift the spectrum upwards. The cone intersects the Fermi energy to form a small Fermi pocket with linear dimension of order x . As shown in Fig. 4(a), the spectral weight is concentrated on one side of the cone, so that only a segment of FS on the side close to the origin carries substantial weight. This is the origin of the notion of “FS segment” introduced in Ref. [34,35].

Now let us see what happens in the SC state when $x_{pc} \neq 0$. Equation (14) takes the standard BCS form if \tilde{E}_{\pm} is interpreted as the normal state dispersion. However, \tilde{E}_{\pm} differs from the normal state spectrum E_{\pm}^N by the appearance of the term $-(x_{pc}\Delta/x)^2$ in Eq. (15). Close to the node this term is small so that qualitatively the spectrum develops from the normal state in a BCS fashion, as shown in Fig. 4(b). This is particularly true

if the higher energy gap between the two branches is smeared by lifetime effects. Thus we see that the “FS segment” is gapped in a BCS-like fashion. However, the velocity v_2 in the $(1, -1)$ direction, being proportional to x_{pc}/x , does not extrapolate to the gap at $(0, \pi)$ (which is essentially independent of x_{pc}), but crosses over to it at the edge of the FS segment. It is worth remarking that in the special case $x_{pc} = x$, $E_{\pm}^{(sc)}$ reduces to the standard BCS form with the normal state dispersion $\varepsilon(\mathbf{k})$, a chemical potential $2\tilde{\mu}$ and a SC gap $\Delta(\mathbf{k})$. The high energy gap closes and spectral weight on one branch vanishes, yielding a BCS spectrum as shown in Fig. 4(c).

We have also calculated the effect of constant \mathbf{A} on the qp dispersion, to linear order of \mathbf{A} . This adds a term $\frac{1}{c}\mathbf{j}_{\pm} \cdot \mathbf{A}$ to Eq. (14) where \mathbf{j}_{\pm} is interpreted as the current carried by the qp. We recall that in standard BCS theory, the current is given in term of the normal state spectrum by $c\partial_{\mathbf{A}}\varepsilon_{\mathbf{A}} = e\partial_{\mathbf{k}}\varepsilon$ because $\varepsilon_{\mathbf{A}}(\mathbf{k}) = \varepsilon(\mathbf{k} + \frac{e}{c}\mathbf{A})$. Remarkably this is almost true in our case in the sense that \mathbf{j}_{\pm} is given by $c\partial_{\mathbf{A}}\tilde{E}_{\pm, \mathbf{A}}$, where $\tilde{E}_{\pm, \mathbf{A}}$ is obtained by replacing \mathbf{k} by $\mathbf{k} + \frac{e}{c}\mathbf{A}$ in ε , $\tilde{\mu}$ and Δ everywhere in Eq. 15 except for the term $(\frac{x_{pc}}{x}\Delta)^2$, which is kept independent of \mathbf{A} . Near the node, $\tilde{\Delta}$ is negligible so that the current is very close to $e\partial_{\mathbf{k}}\tilde{E} \simeq e\partial_{\mathbf{k}}E^N$ (which becomes exactly $e\partial_{\mathbf{k}}\varepsilon$ along the diagonal), thus reproducing Eq. 5. We have checked numerically that even away from the node in the region of the “FS segment”, the current is remarkably close to $e\partial_{\mathbf{k}}E^N$, which can be quite different from the BCS value $e\partial_{\mathbf{k}}\varepsilon$ near the edge of the FS segment.

From Eq. (6), the temperature dependence of the London penetration depth gives a direct measurement of $\alpha^2 \frac{v_F}{v_2}$. Density of states measurements using the T^2 coefficient of the specific heat yields $v_F v_2$. The Fermi velocity can be estimated from transport measurements or high resolution photoemission experiment. Thus in principle the quantities α , v_F and v_2 can be measured. It is of course of great interest to establish how close α is to 1, or whether v_2 is reduced with respect to that extrapolated from the energy gap at $(0, \pi)$ measured by photoemission or tunneling. Crude estimates made in Ref. [27] suggest that α is consistent with 1 but a more precise measurement is clearly called for.

Finally we comment on finite temperature behaviors. In addition to the reduction of superfluid density due to thermal excitation of qp, we expect x_{pc} to decrease with increasing T , leading to a reduction of v_2 : $v_2(T) = \frac{x_{pc}(T)}{x_{pc}(0)}v_2(0)$. As T reaches T_c , $x_{pc} = v_2 = 0$ and the nodes of $E^{(sc)}$ become the “FS segment” while the spin gap near $(0, \pi)$ remain finite. We see that x_{pc} plays the role of the order parameter of the transition, so that we may expect the temperature dependence of x_{pc} to be described by a Ginzburg-Landau theory with X-Y symmetry near the transition.

V. CONCLUSIONS AND OPEN ISSUES

We believe the $SU(2)$ slave boson theory captures the basic physics of the underdoped cuprates. The many anomalous properties associated with the spin gap formation are explained in a natural way. Superconductivity with d -wave pairing symmetry emerges naturally, with quasiparticle excitations which are remarkably similar to BCS theory. However, the microscopic mechanism is completely different in that the SC state is not formed out of pairing of normal state quasiparticles via exchange of some effective interaction. Instead, it is the coherence of the charge degrees of freedom which converts the spin gap phase to the SC state. Many open issues remain, however, and we list a few of them below.

- 1) Our discussion of the electron spectrum in the normal state is still at a crude level. We treat the bosons as “nearly” bose condensed with a relatively narrow spectral function. Thus we do not have a theory of the lineshape. One of the most important features of the photoemission experiment is that a narrow qp peak forms out of a broad lineshape as the SC state develops out of the normal state. We are unable to describe this evolution at present. A narrow spectral line is very natural in the single boson condensation scenario but not as obvious in the boson pair condensation scenario. Thus we have not achieved a quantitative description of the recombination of spin and charge to form quasiparticles in the superconducting state. A related issue is that in our theory the spin gap state and the SC state share the same energy scale, i.e., the energy gap Δ_0 at $(0, \pi)$. Empirically $\Delta_0 \approx J/3$, in rough agreement with the gap calculated in mean field theory. Recently, Shen and collaborators [39] have focused on a higher energy scale (of order J to $2J$) which characterizes the location of the peak in the ARPES spectrum, and argued that it is the peak energy which is smoothly connected with the insulator at half-filling. In this scenario one would need a separate mechanism to produce the leading edge shift and the SC energy gap. In our scenario we have only one energy scale Δ_0 and the burden upon us is to show that the lineshape may exhibit a peak at high energy of order J .
- 2) We do not have a satisfactory theory of the transport of the normal state. This is related to the still lack of understanding of how the spin-charge separation state in the normal state evolves to the well defined qp in the SC. We can only provide a phenomenological picture of gradual binding between holons and spinons to form physical holes as the temperature is decreased. [40]

3) The mean field theory underestimates the spin fluctuation near (π, π) . While inclusion of gauge fluctuations leads to a satisfactory fit of the specific heat and uniform spin susceptibility, [33] it is expected [41] that gauge fluctuations will strongly enhance the spin fluctuation near (π, π) but detailed calculations have not been carried out. This strong enhancement is needed to explain the strong peak in the Cu NMR relaxation at a temperature T^* which is low compared with the spin gap energy Δ_0 . As an intermediate step, we recently carried out a RPA calculation of the spin fluctuation near (π, π) . [42] By tuning a single parameter (the effective exchange coupling in RPA) we are able to account for the resonance peak seen in neutron scattering in the SC state and its evolution with reduced doping. [43] However, at present we cannot explain the neutron scattering and the copper NMR within the same RPA theory.

The work reviewed in this paper has been done in close collaboration with X.G. Wen and I have benefitted from collaboration over the years with N. Nagaosa, T.K. Ng, Derek K.K. Lee, Don H. Kim, and J. Brinckmann. This work was supported by NSF through the MRSEC program DMR 98-08941.

-
- [1] M. Takigawa *et al.*, *Phys. Rev. B* **43**, 247 (1991); for a review see C.P. Slichter, *1993 Los Alamos Symposium Proceedings*.
- [2] J.W. Loram, K.A. Mirza, J.R. Cooper, and W.Y. Liang, *Phys. Rev. Lett.* **71**, 1740 (1993); J.W. Loram, this conference.
- [3] C.C. Homes *et al.*, *Phys. Rev. Lett.* **71**, 1645 (1993); T. Timusk, this conference.
- [4] A.G. Loeser *et al.*, *Science* **273**, 325 (1996).
- [5] H. Ding *et al.*, *Nature* **382**, 51 (1996).
- [6] Ch. Renner *et al.*, *Phys. Rev. Lett.* **80**, 149 (1998).
- [7] A.V. Puchkov *et al.*, *Phys. Rev. Lett.* **80**, 149 (1988).
- [8] J. Orenstein *et al.*, *Phys. Rev. B* **42**, 6342 (1990).
- [9] S. Uchida, J. Low Temp. Phys. 105, (1996).
- [10] S. Tajima, this conference.
- [11] P.W. Anderson, *Science* **235**, 1196 (1987).
- [12] V.J. Emery and S.A. Kivelson, *Nature* **374**, 434 (1995).
- [13] D. Noziers and S. Schmitt-Rink, *J. Low Temp. Phys.* **59**, 195 (1985).
- [14] Y.J. Uemura *et al.*, *Phys. Rev. Lett.* **62**, 2317 (1989); **66**, 2665 (1991).
- [15] C.A.R. Sa de Melo, M. Randeria, and J.R. Engelbrecht, *Phys. Rev. Lett.* **71**, 3202 (1993); *Phys. Rev. B* **55**, 15153 (1997).
- [16] J. Corson, R. Mallozzi, J. Orenstein, J.N. Eckstein, and I. Bozovic, *Nature*, to be published.
- [17] B.O. Wells *et al.*, *Phys. Rev. Lett.* **74**, 964 (1995).
- [18] C. Kane, P. Lee, and N. Read, *Phys. Rev. B* **39**, 6880 (1989).
- [19] A.J. Millis, S.M. Girvin, L.B. Ioffe, and A.I. Larkin, *J. Phys. Chem. Solids* (1998).
- [20] Y. Tokura *et al.*, *Phys. Rev. Lett.* **70**, 2126 (1993).
- [21] M. Grilli and G. Kotliar, *Phys. Rev. Lett.* **64**, 1170 (1990).
- [22] D. Arovas and A. Auerbach, *Phys. Rev. B* **38**, 316 (1988).
- [23] G. Baskaran, Z. Zou, and P.W. Anderson, *Solid State Commun.* **63**, 973 (1987).
- [24] G. Kotliar and J. Liu, *Phys. Rev. B* **38**, 5142 (1988).
- [25] Y. Suzumura *et al.*, *J. Phys. Soc. Jpn.* **57**, 2768 (1988); H. Fukuyama, *Prog. Theo. Phys. Suppl.* **108**, 287 (1992).
- [26] G. Baskaran and P.W. Anderson, *Phys. Rev. B* **37**, 580 (1988); L. Ioffe and A. Larkin, *Phys. Rev. B* **39**, 8988 (1989); P.A. Lee and N. Nagaosa, *Phys. Rev. B* **45**, 966 (1992).
- [27] P.A. Lee and X.G. Wen, *Phys. Rev. Lett.* **78**, 4111 (1997).
- [28] E. Dagotto, *Rev. Mod. Phys.* **66**, 763 (1994).
- [29] R.B. Laughlin, *J. Low Temp. Phys.* **99**, 443 (1995).
- [30] D.A. Bonn *et al.*, *Czech. J. Phys.* **46** S6, 3195 (1996).
- [31] P. Hirschfeld and N. Goldenfeld, *Phys. Rev. B* **48**, 4219 (1993).
- [32] C. Panagopoulos and T. Xiang, *Phys. Rev. Lett.* **81**, 2336 (1998).
- [33] M.U. Ubbens and P.A. Lee, *Phys. Rev. B* **49**, 6853 (1994).
- [34] X.-G. Wen and P.A. Lee, *Phys. Rev. Lett.* **76**, 503 (1996).
- [35] P.A. Lee, N. Nagaosa, T.K. Ng, and X.G. Wen, *Phys. Rev. B* **57**, 6003 (1998).
- [36] I. Affleck, Z. Zou, T. Hsu, and P.W. Anderson, *Phys. Rev. B* **38**, 745 (1988).
- [37] D.H. Kim, P.A. Lee, and X.G. Wen, *Phys. Rev. Lett.* **79** 2109 (1997).
- [38] X.G. Wen and P.A. Lee, *Phys. Rev. Lett.* **80**, 2193 (1998).
- [39] F. Ronning *et al.*, *Science*, to be published.
- [40] D.K.K. Lee and P.A. Lee, *J. Phys. (Cond. Matt.)* **9**, 10421 (1997).
- [41] D.H. Kim and P.A. Lee, *Annals of Physics*, to be published.
- [42] J. Brinckmann and P.A. Lee, preprint.
- [43] H.F. Fong, B. Keimer, D.L. Milius, and Z.A. Aksay, *Phys. Rev. Lett.* **78**, 713 (1997).